Journal of Applied Electrochemistry **33**: 179–186, 2003.

Protection of copper corrosion by carbazole and *N*-vinylcarbazole self-assembled films in NaCl solution

C-T. WANG[1], S-H. CHEN[1,2,*], H-Y. MA[1] and C-S. QI[1]
[1]*Department of Chemistry, Shandong University, Jinan 250100, P.R. China*
[2]*State Key Laboratory for Corrosion and Protection, Shenyang 110015, P.R. China*
*(*author for correspondence, e-mail: shchen@sdu.edu.cn)*

Received 1 May 2002; accepted in revised form 13 December 2002

Key words: carbazole, copper, inhibition efficiency, self-assembled film, *N*-vinylcarbazole

Abstract

Self-assembled films of carbazole (CZ) and *N*-vinylcarbazole (NVC) were prepared on copper surfaces. The corrosion protection abilities of the films were evaluated in an air-saturated 0.5 mol dm^{-3} NaCl solution using electrochemical impedance spectroscopy (EIS), polarization and cyclic voltammetry. The results indicate that CZ and NVC form dense protective films on copper. Fourier transform infrared (FTIR) and X-ray photoelectron spectroscopy (XPS) were used to characterize the film. It was found that the NVC molecules are tilted at an angle to the copper surface. The theoretical *ab initio* calculations support the experimental results.

1. Introduction

Self-assembled films offered by organic substances have advantages for studying the inhibition of metal corrosion because uniform and closely packed films form on the metal surface and provide an insulating layer. Protection of copper from corrosion by self-assembled alkanethiol (R-SH) films has been extensively studied [1–5]. Laibinis and Whitesides described the ability of alkyl thiols to retard the oxidation of a copper surface [1]. Aramaki reported that the maximum copper corrosion protection efficiency for an octadecanethiol self-assembled layer was 80.3% in 0.5 mol dm^{-3} Na_2SO_4 [2]. Self-assembled films of 1-dodecanethiol on copper to protect against corrosion were reported by Feng [4]. Recently, Quan studied the self-assembled films of Schiff bases on copper, which formed by interaction of copper with the nitrogen in the Schiff base molecules [5].

Carbazole (Figure 1(a)) and its derivatives *N*-vinylcarbazole (Figure 1(b)) have found extensive industrial and commercial applications in the manufacture of organic photoconductors and electroluminescence devices [6]. Carbazole and *N*-vinylcarbazole molecules are nitrogen-containing heterocyclic compounds. Polymerization of NVC has been extensively investigated [7]. The self-assembly of carbazole and its derivatives on metal surfaces, however, has not been carried out. Self-assembly of CZ and NVC on copper surfaces was expected to occur in a similar way, since the lone electron pair on the nitrogen atom delocalize with the aromatic rings, allowing the adsorption of CZ and NVC on the copper surface.

The purpose of the present work was to study the protection offered by self-assembled films of CZ and NVC against copper corrosion in NaCl solution. We used electrochemical impedance spectroscopy (EIS), cyclic voltammetry, and polarization to measure the film quality and protection ability. The interaction among the adsorbed molecules was modelled using the Frumkin adsorption isotherm. Spectroscopic techniques, FTIR and XPS, were also used to characterize the orientation of NVC on the copper surface. *Ab initio* calculations were made to provide a theoretical basis for the experimental results.

2. Experimental details

Carbazole and *N*-vinlycarbazole (Fluka, purity $\geqslant$99%) were dissolved in absolute ethanol (AR grade) to the required concentration. An aqueous solution of 0.5 mol dm^{-3} NaCl was prepared by dissolving NaCl in tridistilled water. Copper substrates (10×10 mm, purity 99.9%) were used for FTIR and XPS measurements. The copper electrode was made from a 99.9% pure copper rod with diameter of 5.8 mm. The electrode was embedded in epoxy resin and the exposed surface was polished with 400 and 2000 grit emery papers prior to each experiment.

The electrode was polished, washed with tridistilled water, and then etched in a 7 mol dm^{-3} HNO_3 solution for 30 s [4], rinsed with tridistilled water and absolute ethanol as soon as possible, and immediately immersed in adsorbate solutions to form self-assembled films.

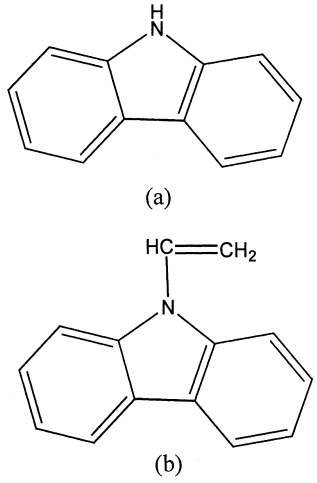

Fig. 1. Structures of (a) carbazole (CZ) and (b) *N*-vinylcarbazole (NVC).

After formation of the film, the electrode was rinsed with ethanol and tridistilled water.

Electrochemical experiments were performed using a three-electrode cell. The reference electrode was a saturated calomel electrode (SCE) and the counter electrodes were platinum plates. All potentials were referred to the SCE. The temperature was 20 ± 2 °C.

EIS measurements, data analysis, potentiostatic polarization and cyclic voltammetry were performed with an IM6 impedance and electrochemical measurement system (Zahner, Germany). The sinusoidal potential perturbation was 5 mV in amplitude and frequencies ranged from 60 kHz to 0.02 Hz. The polarization curves were recorded from −0.4 to 0.1 V vs SCE at a scan rate of 1 mV s^{-1} and cyclic voltammograms were recorded from −0.4 to 0.6 V at a scan rate of 10 mV s^{-1}.

FTIR measurements were recorded using a Nicolet 20SX FTIR spectrometer (USA). Infrared reflection spectra were determined in the mid-infrared region, which extended from 4000 to 400 cm^{-1} at a grazing incidence angle of 86° from the surface normal. The XPS spectra were taken using PHI 5300 ESCA System (Perkin-Elmer, USA). The excitation source was MgK_α radiation (photoelectron energy 1253.6 eV). Take-off angles of 20°, 45° and 70° from the surface were employed. All the analyses were performed at a pressure below 1×10^{-8} torr.

3. Results and discussion

3.1. *EIS measurement*

3.1.1. *Inhibition effect of CZ and NVC self-assembled films*

Electrochemical impedance spectroscopy provides a new method to characterize the film coverage on the electrode, which is related to charge transfer resistance (R_t). The interface capacitance can also be used to determine the film quality [1–5]. It is known that the coverage of an organic substance on the metal surface depends not only on the structure of the organic substance and the nature of the metal, but also on the experimental conditions such as immersion time and concentration of adsorbent [4, 5]. In order to study the influence of these factors on the surface coverage, the following series of experiments was carried out.

The EIS of self-assembled films on copper electrodes were obtained in 0.5 mol dm^{-3} NaCl aqueous solution after 30 min equilibration, since the open-circuit potentials of the electrodes became steady within 30 min. The dependence of open-circuit potentials on equilibration time in 0.5 mol dm^{-3} NaCl solutions is shown in Figure 2. All the impedance spectra were measured at the corresponding open-circuit potentials. Figure 3 shows the impedance plots of copper electrodes in a 0.5 mol dm^{-3} NaCl solution with (b, c) and without (a) films. According to the literature [4, 5], the high-frequency small semicircle in Figure 3(a) is attributable to the time constant of charge-transfer resistance (R_t) and double-layer capacitance (C). The Warburg impedance in the middle and low frequency region is related to the diffusion process of soluble copper species ($CuCl_2^-$) from the electrode surface to the bulk solution [8, 9] or the diffusion of dissolved oxygen from the bulk solution to the electrode surface [10]. Figure 3(b) and (c) are impedance plots of copper electrodes covered by CZ and NVC self-assembled films formed in 1×10^{-3} mol dm^{-3} solution of ethanol with 24 h film formation. Both show larger semicircles than Figure 3(a), which indicates that the charge-transfer step becomes dominant in the corrosion process owing to the formation of self-assembled films on the copper surfaces.

All the impedance spectra were analysed in terms of the equivalent circuits shown in Figure 4. The impedance spectra involving Warburg impedance (Figure 3(a) and (b)) were analysed using the equivalent circuit shown in Figure 4(a). The spectra in Figure 3(c) was fitted in terms of the equivalent circuit Figure 4(b), because the Warburg impedance disappeared and a

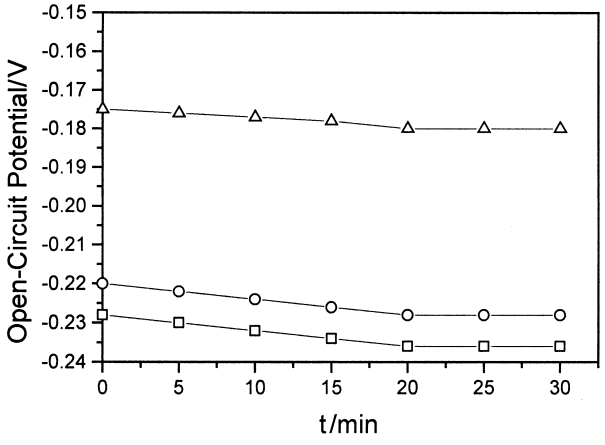

Fig. 2. Time-dependence of open-circuit potentials. Electrodes were equilibrated in 0.5 mol dm^{-3} NaCl solution. Key: (□) NVC-covered copper; (○) CZ-covered copper; (△) bare copper.

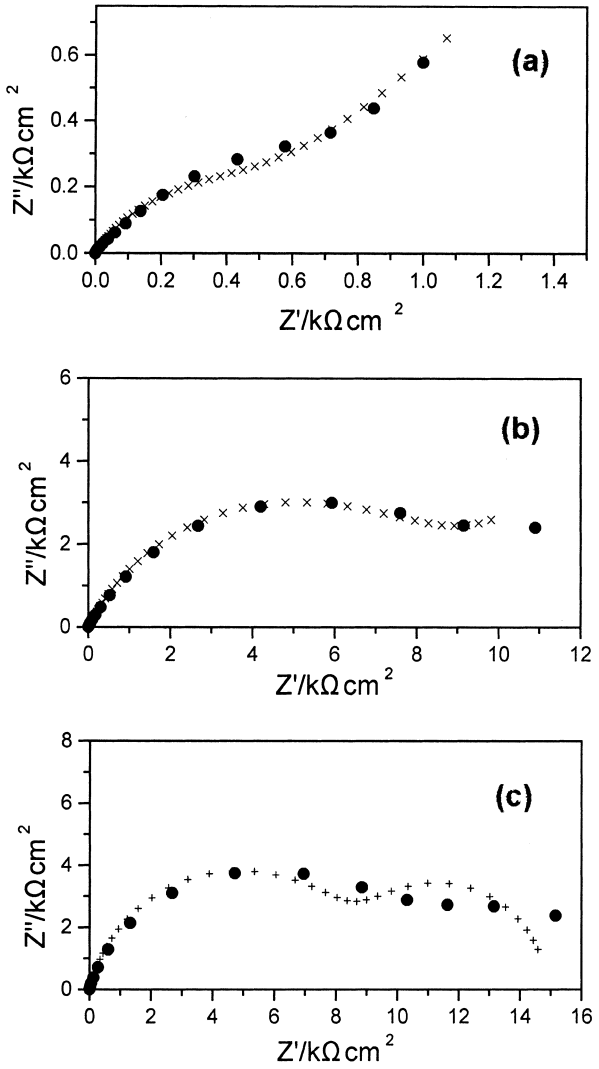

Fig. 3. Nyquist impedance diagrams in 0.5 mol dm^{-3} NaCl solutions for Cu electrodes with and without self-assembled films of CZ and NVC. (a) bare copper, $E_{corr} = -0.236$ V, (b) CZ film, $E_{corr} = -0.228$ V, (c) NVC film, $E_{corr} = -0.180$ V. Key: (●) measured; (×) fitted.

second time constant was observed in Figure 3(c). In the circuits, W stands for the Warburg impedance, R_t the charge-transfer resistance, R_s the solution resistance and R_a the pseudo-resistance. In addition, a constant phase element (CPE) was used as a substitute for the capacitor to fit the impedance behaviour of the electric double-layer more accurately, since the high-frequency semicircles measured were not regular but depressed because of a dispersing effect [10]. CPE is described by two parameters, the capacitance and an exponent n, according to IM6 impedance analysis. Fitted and measured curves are both displayed in Figure 3, and coincide well. According to the fit, the bare copper electrode had the parameters of $R_t = 0.549$ kΩ cm^2, $C = 20.13$ μF cm^{-2}, $n = 0.642$. When covered with CZ and NVC film, the R_t increased to 9.09 and 10.15 kΩ cm^2, C decreased to 4.068 and 2.635 μF cm^{-2} and n increased to 0.712 and 0.862, respectively.

The film coverage (θ) on the metal surface can be calculated using [11]

$$(1 - \theta) = R_t^o / R_t \quad (1)$$

where R_t^o and R_t are the charge–transfer resistance of the bare copper electrode and the film covered electrode, respectively. The coverage of CZ and NVC are 93.5% and 94.2%, respectively. The NVC film has higher R_t, lower C, higher n and higher coverage than CZ, indicating the NVC film had higher quality than the CZ film.

3.1.2. *Effects of the immersion time on film formation*

A series of EIS corresponding to different immersion time were measured from 2 s to 28 h. The coverages were calculated using Equation 1. Figure 5 shows the dependence of the surface coverage for CZ and NVC on immersion time. In the case of NVC, in the initial 30 minutes, the coverage increased markedly, and then tended to stay at a constant value of 0.94. This result indicates that the formation process of the self-assembled film can be classified into two steps, fast adsorption at the beginning and then a slow rearrangement, as

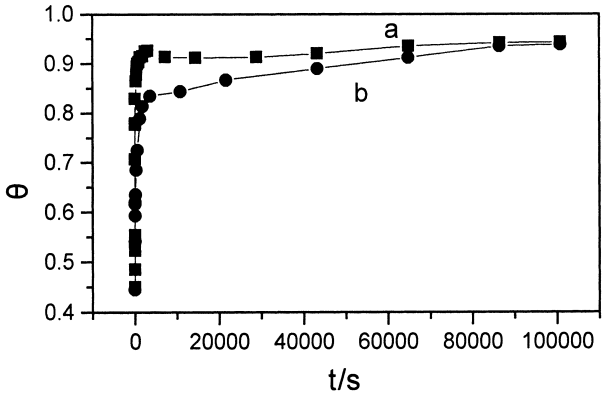

Fig. 5. Dependence of the surface coverage of CZ (a) and NVC (b) on the immersion time.

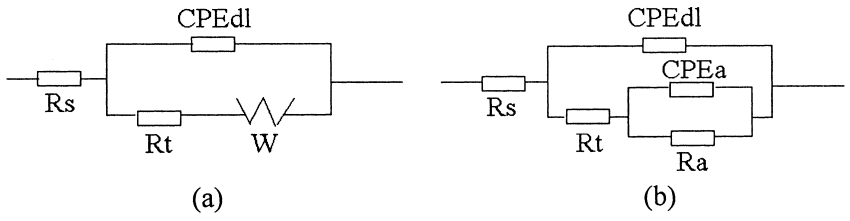

Fig. 4. Equivalent circuits used to fit impedance spectra in Figure 2.

described by Rondelez and coworkers [12]. With increase in immersion time, the film becomes denser and more stable. The CZ results are similar to the NVC results, but the saturated adsorption time was longer than that of NVC. To obtain a dense and stable self-assembled film, the best immersion time was determined to be more than 20 h. So we consider that the saturated adsorption time is about 24 h, which is identical with the experimental result of Quan for Schiff base adsorption on copper [5].

3.1.3. *Application of the Frumkin adsorption isotherm*

Over a long assembling time, such as 24 h, the adsorption of CZ and NVC shows equilibrium characteristics. EIS of CZ and NVC in concentration from 10^{-3} to 10^{-7} mol dm^{-3} were measured. Using the coverage obtained from Equation 1, the experimental data were fitted to the Langmuir adsorption isotherm equation first, but $1/(1-\theta)$ against concentration was not linear. The adsorption of CZ and NVC on Cu were then modelled using the Frumkin adsorption isotherm equation [13]

$$\ln\left[\frac{\theta}{c(1-\theta)}\right] = \ln K + 2a\theta \qquad (2)$$

where K is the constant of the adsorption equilibrium including the adsorption free energy and a is the attraction constant characterizing the lateral interaction among the molecules [13]. The experimental data match the Frumkin adsorption isotherm (shown in Figure 6) very well. From the intercept of the lines at $\theta = 0$, the adsorption free energies (ΔG_{ads}) were calculated. The ΔG_{ads} of CZ is -33.7 kJ mol^{-1}, which is close to the value of 3-mercaptopropylthiomethoxysilane (MPS), -35 kJ mol^{-1} [14]. The value of NVC is -42.6 kJ mol^{-1}, more negative than both MPS and CZ. These adsorption processes can be considered as chemisorption processes because the adsorption free energy is more negative than -25 kJ mol^{-1} [13]. Based upon the ΔG_{ads} values, the chemisorption processes are related to adsorption processes that take place through the lone pair electrons of the nitrogen and the delocalized π-electrons of the aromatic ring. The higher value ΔG_{ads} for NVC is due to the presence of the vinyl substituent group, which increases the delocalization effect of the aromatic ring. The attraction constant $a < 0$ indicates that the adsorbed molecules attract one another. This driving force may improve the adsorption rate and the stability of the films.

3.2. *Polarization measurement*

Figure 7 shows the polarization curves for copper with and without self-assembled films of CZ and NVC. The experimental conditions were identical with the EIS measurements in Figure 3. For the bare copper electrode (Figure 7(a)), a linear relation is observed in the active dissolution region. The existence of a Tafel slope is indicative of an electrode reaction controlled by charge transfer. At high anodic potentials (around 0 V), a current hump was caused by CuCl precipitation [15].

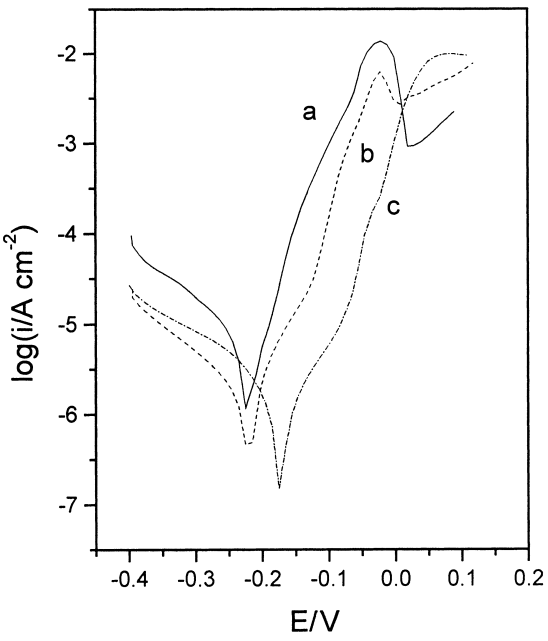

Fig. 7. Polarization curves obtained in 0.5 mol dm^{-3} NaCl. (a) Bare copper, (b) covered with CZ, (C) covered with NVC.

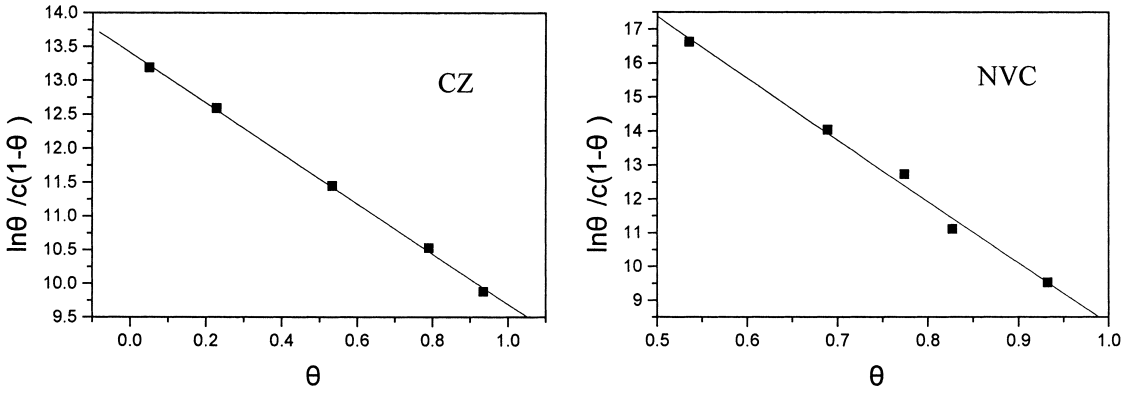

Fig. 6. Frumkin adsorption isotherm of CZ and NVC on copper.

The lower anodic and cathodic current seen in Figure 7(b) and (c), implies that the films inhibit both anodic and cathodic electrochemical processes. That is, both films increase the charge-transfer resistance of anodic dissolution of copper, slowing down the corrosion rate of copper in solution; meanwhile, the CZ and NVC films act as barriers to the diffusion of oxygen molecules from the solution to the copper electrode, which may increase the overpotential for cathodic reduction of dissolved oxygen. In addition, the corrosion potential of the copper electrode shifted positively after it was covered by a NVC film, indicating that the film inhibits the anodic dissolution of copper much more than the cathodic reduction of dissolved oxygen. These results are consistent with those obtained from EIS.

Corrosion current densities (i_{corr}) were determined from the polarization curves by extrapolating the Tafel lines to the corrosion potentials. For bare copper, the i_{corr} value was 7.1 μA cm^{-2} (Figure 7(a)). For the CZ and NVC film-covered copper, the i_{corr} values were 0.65 μA cm^{-2} (Figure 7(b)) and 0.47 μA cm^{-2} (Figure 7(c)), respectively. The percentage inhibition efficiency (P) was calculated by the following formula:

$$P = \frac{i^{o} - i}{i^{o}} \times 100 \qquad (3)$$

where i^{o} and i are the corrosion current densities for the bare copper electrode and the film covered electrode, respectively. For CZ, the inhibition efficiency against copper corrosion is 91.1%; while for NVC, it is 93.4%.

3.3. *Cyclic voltammetry*

Figure 8 shows cyclic voltammograms of a NVC film covered and a bare copper electrode in 0.5 mol dm^{-3} NaCl solution. For the bare copper electrode, three anodic peaks and one cathodic peak are observed. The peak (a) represents the anodic reaction from Cu to CuCl, peak (b) refers to the formation of $CuCl_2^-$, peak (c) corresponds to the reaction of $CuCl_2^-$ to CuCl, and peak (d) represents the process of reduction from CuCl to Cu. For the electrode with the NVC self-assembled film, the oxidation peaks (a), (b), (c) and the reduction peak (d), are smaller than those of the bare electrode. These results indicate that the film inhibits the oxidation of the copper substrate and limits the following reduction reaction. The peak (b) decreases much more than peak (a) does, which may be caused by the difficulty of Cl^- diffusion to the copper surface owing to repulsion by the negative charge on the aromatic rings. After 10 cycles, the cyclic voltammograms were invariable, indicating that the film is stable in the potential region from −0.6 to 0.4 V.

3.4. *XPS, FTIR analysis*

XPS spectra of NVC film covered copper were performed to obtain more detailed information about the adsorption. The film was prepared from an ethanol solution with a 24 h immersion time. Using a 45° take-off angle, the elements Cu, C, N, O were detected. And the surface atomic compositions were Cu 3.30, C 65.62, N 2.57 and O 28.51. Figure 9 shows the XPS spectra of Cu $2p_{3/2}$ and N 1s for NVC film-covered copper and the Cu LMM Auger spectra of copper covered with NVC film, which was obtained after the copper substrate was immersed in a 1 mmol dm^{-3} NVC solution for 24 h. The Cu $2p_{3/2}$ peak at a binding energy (BE) of 932.5 eV could be attributed to either metallic copper or Cu(I), which was hardly distinguishable in the Cu 2p spectra (0.1 eV BE shift). Cu(II) which should be located at a BE of 933.5 eV was not found in the spectra [4]. The presence of a N 1s peak at 409.2 eV provided evidence that the NVC was really adsorbed on the copper surface. The Cu LMM Auger spectra of copper covered with a NVC film shows the existence of both Cu(O) and Cu(I), which are located at 335.0 and 337.0 eV, respectively. The Auger peak at 337.0 eV is very small, compared with the peak of metallic copper at 335.0 eV, indicating

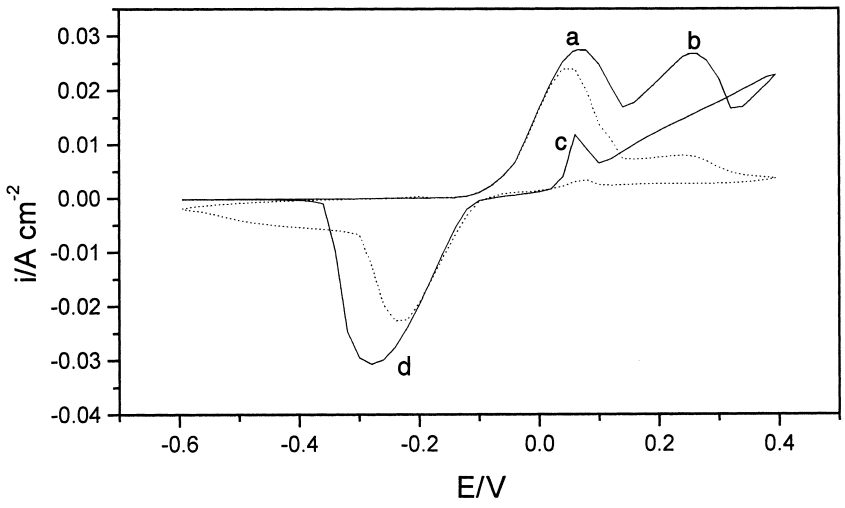

Fig. 8. Cyclic voltammograms of NVC film covered (dotted line) and bare copper (solid line).

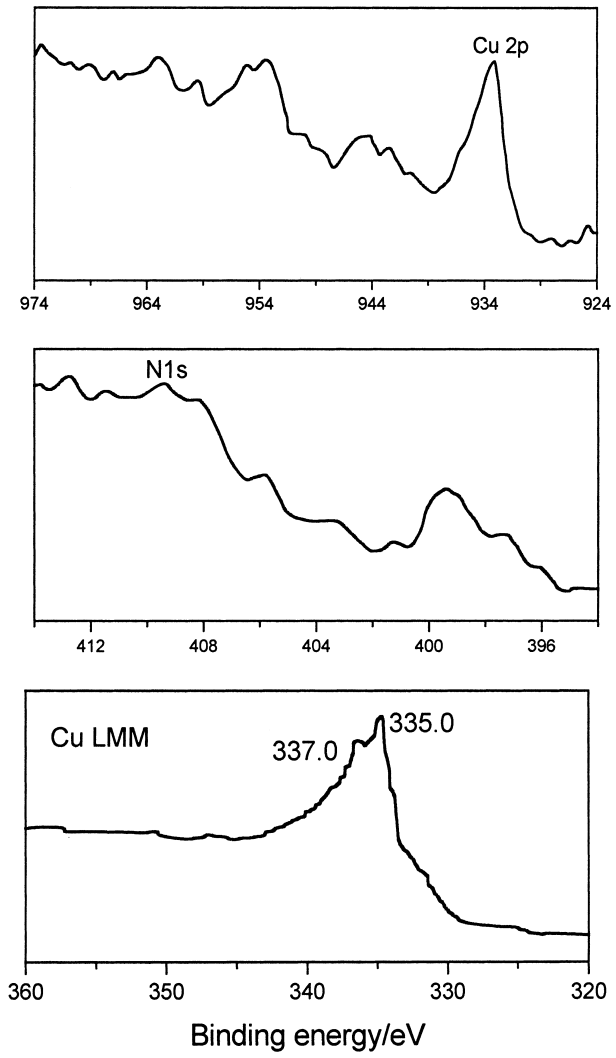

Fig. 9. XPS spectra of Cu 2p and N 1s for NVC self-assembled film on Cu and Cu LMM Auger spectra of copper covered with NVC film by 24 h immersion in 10^{-3} mol dm^{-3} NVC solution.

Table 1. Atomic percentage for a NVC film covered copper with different take-off angles by XPS analysis

Take of angles	20°	45°	70°
Cu	4.70	3.30	2.96
C	67.56	65.62	64.33
O	25.92	28.51	30.05
N	1.82	2.57	2.67

that little cuprous oxide was introduced during the preparation of the film. The existence of oxygen in the film showed that oxygen dissolved in the solution had taken part in the self-assembly process, either oxidizing some of the Cu atoms on the substrate surface or promoting the NVC adsorption on the copper surface, which is similar to the adsorption of thiols on Au surface [16]. To determine the interaction between the copper surface and NVC molecules, the atomic percentage of the NVC film covered copper was measured using different take-off angles. The results are listed in Table 1. It can be seen that the atomic percentage of N increases with increase in the take-off angles, which suggest that NVC molecules link to the copper surface by the formation of Cu–N bonds.

The FTIR reflection spectrum of NVC film adsorbed on copper is shown in Figure 10. Bands appearing at 1634.7, 958.52 and 853.52 cm^{-1} indicate the $-CH{=}CH_2$ stretching modes, 1226.8 cm^{-1} is the C–N stretching vibration, and 1446.9 cm^{-1} arises from the framework vibration of the aromatic rings. This provides a further demonstration that the NVC is adsorbed onto the copper surface. Moreover, from this information we can determine the orientation of the molecules adsorbed on the surface. The surface selection rule states that dynamic dipoles parallel to the surface are very strongly screened such that those corresponding modes are not

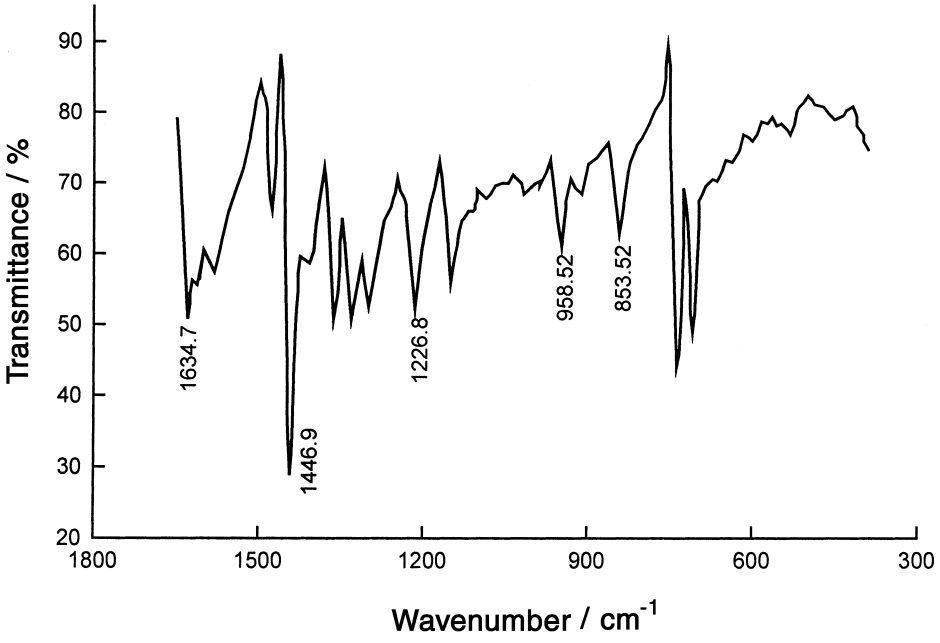

Fig. 10. Fourier transform infrared (FTIR) spectra of NVC film on copper.

observed [17]. The observation of the framework vibration of the aromatic rings at 1446 cm^{-1} indicates that the aromatic rings do not adopt an absolutely flat orientation, but rather are tilted relative to the copper surface. Although aromatic rings can adsorb on most metal surfaces in a flat-lying geometry with the molecular plane parallel to the surface [18], in the case of NVC, competition between the π-donation by the aromatic rings and electron-donation by the nitrogen atom affects the orientation of the molecule, changing it from lying flat to tilting away from the copper surface.

3.5. *Quantum chemical calculations*

To obtain further insight into the adsorbent–surface interaction, *ab initio* quantum chemical calculations were performed not only for CZ, but also for NVC. The corresponding molecular geometries were optimized and the energies were calculated at HF/LANL2DZ level.

According to Fukui's frontier orbital approximation [19], interactions occur only between frontier MO (Molecular Orbitals), HOMO (highest occupied molecular orbital) and LUMO (lowest unoccupied molecular orbital) of both reactants. It is known that a metal can accept electrons from electron donors into its lowest unoccupied orbital. Vosta pointed out that the higher the HOMO energy of the adsorbent molecule, the stronger the bonding between the adsorbent and the surface [20, 21]. Our calculations showed that the HOMO energy (−743.6 kJ mol^{-1}) of NVC was higher than that of CZ (−754.7 kJ mol^{-1}). Also the LUMO energy (230.68 kJ mol^{-1}) of NVC was lower than that of CZ (245.7 kJ mol^{-1}). These results provide a theoretical confirmation that NVC has stronger bonding affinity for copper than CZ, which is consistent with the experimental results obtained from EIS and polarization curves.

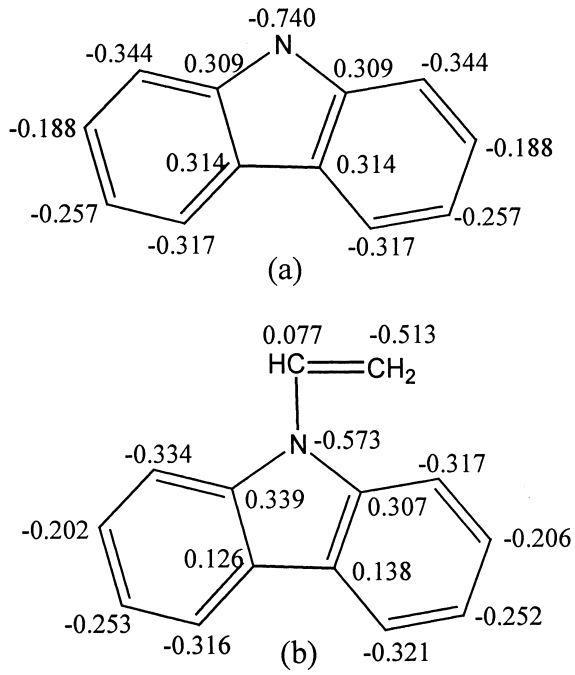

Fig. 11. Total atomic charges of (a) carbazole (CZ) and (b) *N*-vinylcarbazole (NVC) molecules obtained by *ab initio* quantum calculations.

It is confirmed that the more negative the atomic charges of the adsorbed centre, the more easily the atom donates its electrons to the metal unoccupied orbital. In Figure 11, the atomic charges of the nitrogen atom are −0.740 for CZ and −0.573 for NVC, respectively, more negative than any C atoms in their corresponding molecule, offering evidence that CZ and NVC must anchor to the copper surface through the nitrogen atoms, leaving an angle between the molecular plane and the copper surface, which is in agreement with the results of the XPS and FTIR experiments.

4. Conclusion

Self-assembled films of CZ and NVC were prepared on copper surfaces. These films offered significant protection against copper corrosion in neutral aqueous NaCl solution. The inhibition efficiencies of CZ and NVC, determined by polarization measurements, were 91.1 and 93.4%, respectively. Increased immersion time improve the quality of the self-assembled films. The adsorption processes of CZ and NVC both obey the Frumkin adsorption isotherm. Moreover, surface analyses by XPS and FTIR confirmed the fact of CZ and NVC adsorption on the copper surface. NVC molecules link to the copper surface through a Cu-N bond, producing a tilted orientation from the copper surface. *Ab initio* quantum calculations provide a theoretical explanation for the electrochemical, XPS and FTIR experimental results.

Acknowledgements

This work was supported by the Special Funds for Major State Basic Research Projects (G19990650) and the Chinese National Science Fund (No. 20173033).

References

1. P.E. Laibinis and G.M. Whitesides, *J. Am. Chem. Soc.* **114** (1992) 9022.
2. Y. Yamamoto, H. Nishihara and K. Aramaki, *J. Electrochem. Soc.* **140** (1993) 436.
3. R. Haneda and K. Aramaki, *J. Electrochem. Soc.* **145** (1998) 2786.
4. Y. Feng, W.K. Teo, K.S. Siow, Z. Gao, K.L. Tan and A.K. Hsieh, *J. Electrochem. Soc.* **144** (1997) 55.
5. Z. Quan, X. Wu, S. Chen, S. Zhao and H. Ma, *Corrosion* **57** (2001) 195.
6. J. Bisberg, W.J. Cuming, R.A. Gaudiana, K.D. Hutchinson, R.I. Ingwall, E.S. Kolb, P.G. Mehta, R.A. Minns and C.P. Petersen, *Macromolecules* **28** (1995) 386.
7. C.J. Lee, D.H. Kim, J.M. Oh, K.H. Park, N. Kim, B.C. Ji and W.S. Ly, *J. Appl. Polym. Sci.* **76** (2000) 1558.

8. H.P. Lee and K. Nobe, *J. Electrochem. Soc.* **133** (1986) 2035.
9. Y. Feng, K.S. Siow, W.K. Teo and A.K. Hsieh, *Corrosion* **53** (1997) 389.
10. H. Ma, S. Chen, L. Niu, S. Zhao, S. Li and D. Li, *J. Appl. Electrochem.* **32** (2002) 65.
11. J. Wang, B. Zeng, C. Fang and X. Zhou, *Anal. Sci.* **16** (2000) 457.
12. J.B. Brzoska, N. Shahidzadeh and F. Rondelez, *Nature* **360** (1992) 719.
13. E. Geler and D.S. Azambuja, *Corros. Sci.* **42** (2000) 631.
14. R. Tremont, H.D. Jesus-Cardona, J. Garcia-Orozco, R.J. Castro and C.R. Cabrera, *J. Appl. Electrochem.* **30** (2000) 737.
15. A.L. Bacarell and J.C. Griess, *J. Electrochem. Soc.* **120** (1973) 459.
16. C. Schoenenberger, J.A.M. Sondag-Huethorst, J. Jorritsma and L.G.J. Fokkink, *Langmuir* **10** (1994) 611.
17. D. Syomin, J. Wang and B.E. Koel, *Surf. Sci.* **495** (2001) 827.
18. J.H. Kang, R.L. Toomes, J. Robinson, D.P. Woodruff, O. Schaff, R. Terborg, R. Lindsay, P. Baumgartel and A.M. Bradshaw, *Surf. Sci.* **448** (2000) 23.
19. H. Fujimoto, S. Kato, S. Yamabe and K. Fukui, *J. Chem. Phys.* **60** (1974) 572.
20. J. Vosta, J. Eliasek and P. Knizek, *Corrosion* **32** (1976) 183.
21. J. Vosta and N. Hackerman, *Corros. Sci.* **30** (1990) 949.